JOC The Journal of Organic Chemistry

Article

Cite This: J. Org. Chem. 2019, 84, 2568−2576

pubs.acs.org/joc

Sarcomililate A, an Unusual Diterpenoid with Tricyclo[11.3.0.0^{2,16}]hexadecane Carbon Skeleton, and Its Potential Biogenetic Precursors from the Hainan Soft Coral *Sarcophyton mililatensis*

Min Yang,[†,‡,⊥] Xiao-Lu Li,[§,⊥] Jian-Rong Wang,[†] Xinxiang Lei,[∥] Wei Tang,[†] Xu-Wen Li,*[,†,‡] Han Sun,*[,§] and Yue-Wei Guo*[,†,‡,#]

[†]State Key Laboratory of Drug Research, Shanghai Institute of Materia Medica, Chinese Academy of Sciences, 555 Zu Chong Zhi Road, Zhangjiang Hi-Tech Park, Shanghai 201203, P. R. China

[‡]University of Chinese Academy of Sciences, No. 19A Yuquan Road, Beijing 100049, P. R. China

[§]Leibniz-Forschungsinstitut für Molekulare Pharmakologie (FMP), Robert-Rössle-Str. 10, Berlin 13125, Germany

[∥]School of Pharmaceutical Sciences, South Central University for Nationalities, Wuhan 430074, P. R. China

[#]College of Pharmaceutical Sciences, Zhejiang University of Technology, Hangzhou 310014, P. R. China

Supporting Information

ABSTRACT: A novel diterpenoid, sarcomililate A (**1**), possessing a previously undescribed tricyclo[11.3.0.0^{2,16}]hexadecane scaffold, along with two new cembranoids, sarcomililatols A and B (**2** and **3**), and two known related diterpenoids (**4** and **5**), was isolated from the Hainan soft coral *Sarcophyton mililatensis*. The complete chemical structure including absolute configuration (AC) of **1** was unambiguously determined by a combination of residual dipolar coupling (RDC)-based NMR analysis, TDDFT-ECD (ECD = electronic circular dichroism) calculation, and Snatzke's method. The AC of **1** was further confirmed by a comparison with **2**, whose AC was determined by anomalous X-ray diffraction. A plausible biogenetic relationship of **1**−**3** was further proposed. All the reported compounds exhibited interesting inhibitory effects on the ConA-induced T lymphocytes and/or lipopolysaccharide (LPS)-induced B lymphocytes proliferation.

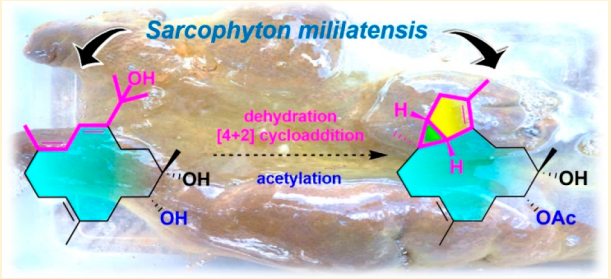

INTRODUCTION

Soft corals of the genus *Sarcophyton* (order *Alcyonacea*, family *Alcyoniidae*) are abundant species in the South China Sea. They have been proven to be rich sources for diterpenoids with intriguing structural features and promising biological activities ranging from antitumoral, antibacterial, to enzyme inhibitory effects.[1] Our previous studies on several Hainan *Sarcophyton* soft corals have led to the isolation and identification of a number of new cembranoids as main metabolites.[2−7] Furthermore, several diterpenoids with unprecedented carbon skeletons were recently discovered.[8−10]

In this study, the Hainan soft coral *Sarcophyton mililatensis* collected off Xigu Island, Hainan Province, China, was chemically investigated for the first time, resulting in the discovery of three new and two known diterpenoids **1**−**5** (Figure 1). Among them, sarcomililate A (**1**) represents the first example of natural products containing an unprecedented tricyclo[11.3.0.0^{2,16}]hexadecane core. While the constitution of **1** was established by conventional spectroscopic methods, determination of relative and absolute configuration turned out to be particularly challenging as it was noncrystallizable and two stereochemical domains cannot be connected by NOEs and *J*-couplings. Herein, we employed residual dipolar coupling (RDC)-based NMR spectroscopy for establishing the relative configuration of five unknown stereocenters of **1**. RDC provides valuable structural information about the relative orientation between the internuclear vectors, which are not sensitive to breaks in the scalar or NOE connectivity. This is of special importance in the context of configurational assignments of unknown stereogenic units that are distant to each other. Therefore, in recent years RDC-based anisotropic NMR spectroscopy has emerged as an important technique for the determination of constitution, conformation, and relative configuration of structurally challenging natural products.[11−16] Comparison of experimental and theoretically calculated electronic circular dichroism (ECD) spectra permitted the assignment of the absolute configuration of **1**, which was finally approved by a comparison with co-occurring sarcomililatol A

Received: November 26, 2018
Published: February 5, 2019

DOI: 10.1021/acs.joc.8b03020
J. Org. Chem. 2019, 84, 2568−2576

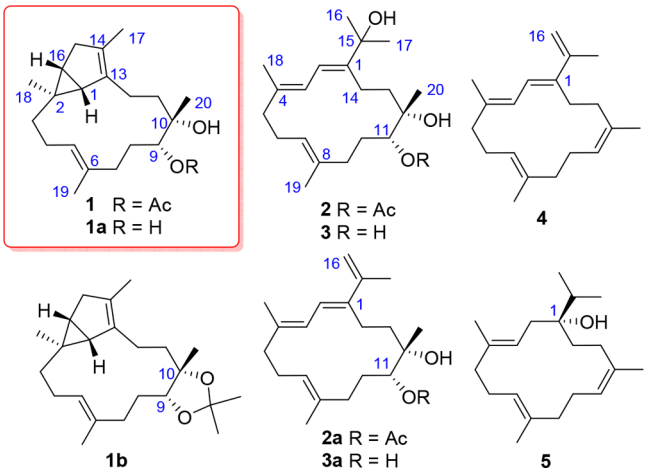

Figure 1. Structures of the isolates and their derivatives.

(**2**), whose absolute configuration was established by anomalous X-ray diffraction.

RESULTS AND DISCUSSION

Sarcomililate A (**1**), a colorless oil, was assigned with the molecular formula $C_{22}H_{34}O_3$ by the HR-EI-MS at *m/z* 346.2507 (calcd 346.2508), indicating six degrees of unsaturation. The IR spectrum of **1** displayed characteristic absorptions indicative of ester carbonyl (ν_{max} 1733 cm^{-1}) and hydroxyl (ν_{max} 3456 cm^{-1}). Its ^{13}C NMR spectrum (Table 1) combining HSQC experiment disclosed 22 carbon resonances, including five methyls, seven sp^3 methylenes, three sp^3 methines (an oxygenated one at δ_C 79.9), two sp^3 quaternary carbons (an oxygenated one at δ_C 73.9), one sp^2 methine (an olefinic carbon at δ_C 125.4), and four sp^2 quaternary carbons (an ester carbonyl at δ_C 170.1 and three olefinic carbons at δ_C 135.1, 134.4, and 132.4). An ester carbonyl and two double bonds accounted for three of the total six degrees of unsaturation, implying the presence of a tricyclic ring system in **1**.

The extensive analysis of $^1H-^1H$ COSY spectrum of **1** defined four spin systems **a**–**d** (Figure 2), by clear correlations of H-1 (δ_H 1.73)/H-16 (δ_H 1.04)/H_2-15 (δ_H 2.42, 1.98) (**a**); H_2-3 (δ_H 1.88, 0.76)/H_2-4 (δ_H 2.37, 2.02)/H-5 (δ_H 5.33) (**b**); H_2-7 (δ_H 2.38, 2.10)/H_2-8 (δ_H 2.10, 1.73)/H-9 (δ_H 5.02) (**c**); and H_2-11 (δ_H 1.67, 1.51)/H_2-12 (δ_H 2.35, 1.91) (**d**), respectively. Fragment **a** was connected with two singlet methyls at δ_C 13.1 and 10.0 and three quaternary carbons at δ_C 135.1, 132.4, and 23.0, by careful interpretation of the well-resolved HMBC correlations from H-1/H_2-15 (δ_H 2.42, 1.98) to C-14 (δ_C 132.4), from H-16 to C-13 (δ_C 135.1)/C-14, from

Table 1. ^1H and ^{13}C NMR Data of 1[a] Recorded in Different Deuterated Solvents[b]

position	δ_C in CD_3OD[c]	δ_C in C_6D_6[d]	δ_C in $CDCl_3$[e]	position	δ_H (mult, *J* in Hz) in CD_3OD[c]	δ_H (mult, *J* in Hz) in C_6D_6[d]
1	43.0	42.5	42.2		1.71 (dd, 7.0, 2.3)	1.74 (dd, 6.7, 2.8)
2	23.2	23.0	22.9			
3	39.5	39.1	38.7	**3a**	1.92 (m)	1.88 (dt, 13.8, 4.1)
				3b	0.87 (m)	0.76 (m)
4	26.1	25.6	25.3	**4a**	2.38 (m)	2.37[f] (m)
				4b	2.08 (m)	2.02 (m)
5	125.7	125.4	125.2		5.32 (t, 6.5, 6.5)	5.33 (dd, 9.7, 4.6)
6	134.9	134.4	134.4			
7	35.9	35.6	35.2	**7a**	2.27[f] (m)	2.38[f] (m)
				7b	1.94[f] (m)	2.10[f] (m)
8	28.7	28.4	28.1	**8a**	1.74 (m)	2.10[f] (m)
				8b	1.99 (m)	1.73 (m)
9	80.6	79.9	80.2		4.94 (dd, 7.0, 2.7)	5.02 (dd, 5.5, 3.5)
10	74.8	73.9	74.2			
11	37.7	37.0	36.4	**11a**	1.66[f] (m)	1.67 (m)
				11b	1.39 (m)	1.51[f] (m)
12	24.4	23.5	23.2	**12a**	1.82 (t, 12.7, 12.7)	2.35[f] (m)
				12b	2.29[f] (m)	1.91 (m)
13	135.7	135.1	134.4			
14	132.8	132.4	132.9			
15	38.3	37.9	37.6	**15a**	1.95[f] (m)	2.42 (dd, 18.1, 7.9)
				15b	2.42 (dd, 18.0, 7.9)	1.98 (dd, 18.1, 1.3)
16	25.8	25.4	25.0		1.02 (td, 7.0, 7.0, 0.8)	1.04 (ddd, 7.9, 6.7, 1.3)
17	12.9	13.1	13.2		1.54, 3H (s)	1.50, 3H (s)
18	10.6	10.0	10.0		0.71, 3H (s)	0.75, 3H (s)
19	17.1	16.8	16.8		1.66, 3H (s)	1.62, 3H (s)
20	23.5	24.3	24.3		1.11, 3H (s)	1.08, 3H (s)
C═O	172.8	170.1	170.9			
$COCH_3$	20.9	20.7	21.4		2.09, 3H (s)	1.69, 3H (s)

[a]Assignments were deduced by analysis of 1D and 2D NMR spectra. [b]Compound **1** could slightly degrade in $CDCl_3$ when recording the 2D NMR spectra; thus, C_6D_6 and CD_3OD were used to record the full NMR spectra. [c]Bruker DRX-600 spectrometer (150 MHz for ^{13}C NMR and 600 MHz for ^1H NMR); chemical shifts (ppm) referred to CH_3OH (δ_C 49.00; δ_H 3.31). [d]Bruker DRX-500 spectrometer (125 MHz for ^{13}C NMR) in C_6D_6; Bruker DRX-400 spectrometer (400 MHz for ^1H NMR) in C_6D_6; chemical shifts (ppm) referred to C_6H_6 (δ_C 128.06; δ_H 7.16). [e]Bruker DRX-500 spectrometer (125 MHz for ^{13}C NMR); chemical shift (ppm) referred to $CHCl_3$ (δ_C 77.16). [f]Overlapped.

DOI: 10.1021/acs.joc.8b03020
J. Org. Chem. 2019, 84, 2568–2576

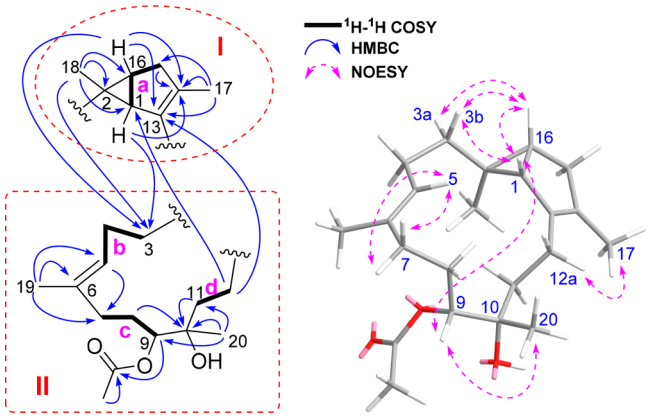

Figure 2. ^{1}H−^{1}H COSY and key HMBC and NOESY correlations of **1**.

H_3-17 (δ_H 1.50) to C-13/C-14/C-15 (δ_C 37.9), and from H_3-18 (δ_H 0.75) to C-1 (δ_C 42.5)/C-2 (δ_C 23.0)/C-16 (δ_C 25.4), leading to the construction of a partial structure **I**, a bicyclo[3.1.0]hexane skeleton (Figure 2). Subunits **b**−**d**, bearing in mind the remaining three singlet methyls (δ_C 24.3, 20.7, and 16.8) and three quaternary carbons (δ_C 170.1, 134.4, and 73.9), were connected by interpretation of the clear HMBC cross-peaks from H_3-19 (δ_H 1.62) to C-5 (δ_C 125.4)/C-6 (δ_C 134.4)/C-7 (δ_C 35.6), from H-5 to C-7, from H_2-8/H_2-11/H_3-20 (δ_H 1.08) to C-10 (δ_C 73.9), from H_3-20 to C-9 (δ_C 79.9)/C-10/C-11 (δ_C 37.0), and from H-9/9-$COCH_3$ (δ_H 1.69) to 9-$COCH_3$ (δ_C 170.1), forming a linear partial structure **II**, bearing an acetoxy group at C-9 and a hydroxy group at C-10. Finally, the HMBC cross-peaks from H-1/H-16/H_3-18 to C-3 (δ_C 39.1), and from H_2-12 to C-1/C-13, clearly indicated that the two ends (C-3 and C-11) of the partial structure **II** were connected to the C-2 and C-13 of fragment **I**, forming a tricyclo[11.3.0.0^{2,16}]hexadecane skeleton (**1**) that has not been discovered before in any known diterpenoid (Figure 2).

The geometry of the olefins at C-5 and C-13 of **1** was easily elucidated by NOESY experiment (Figure 2). The clear NOE correlations between H-5 and H_2-7 (δ_H 2.38, 2.10) and the lack of correlation between H-5 and H_3-19 indicated *E* configuration of $\Delta^{5,6}$, whereas the *Z* configuration of $\Delta^{13,14}$ was determined by the NOE correlation between H_3-17 and H-12a (δ_H 2.35). There are five undefined asymmetric centers (C-1, C-2, C-9, C-10, and C-16) in **1**, resulting in 16 possible relative configurations. Although some key NOE correlations among the protons of the chiral carbons have been observed as shown in Figure 2, determination of the relative configuration between two distant stereochemical domains C-1/C-2/C-16 and C-9/C-10 was not possible by conventional NMR-based method, as they are separated by four bonds and only one NOE (H-1 and H-9, Figure 2) could be detected between these two domains. Moreover, ambiguity exists regarding the relative configuration of C-9 and C-10 in the 13-membered macrocycle. To tackle this problem, we decided to perform RDC-based NMR analysis to assign the relative configuration of **1**.

For acquiring the RDC data, we aligned **1** in a self-assembled oligopeptide (AAKLVFF) phase, which has been recently proposed as a liquid crystalline-based alignment medium that is compatible with MeOH.[17] Altogether we were able to extract 14 $^1D_{CH}$ values ranging from −55.3 to 43.5 Hz with high accuracy using [^{1}H−^{13}C]-CLIP-HSQC spectra (Figure S2).[18] These 14 $^1D_{CH}$ contain valuable information regarding the internuclear proton-carbon or methyl orientation of all unknown stereocenters.

For the RDC fitting, we sampled the conformational space of 16 possible configurations using the conformational search method implemented in the program by Schrödinger.[19] After energy minimization, only 10 configurations (Table 2) were found to be stable. A careful *J*-coupling analysis using the data from ^{1}H,^{1}H-ECOSY, ^{1}H,^{13}C-HSQMBC, and ^{1}H,^{13}C-HECADE experiments suggested a single dominant conformer around the dihedrals C-2/C-3, C-3/C-4, C-4/C-5, C-6/C-7, C-7/C-8, C8−C9, and C-11/C-12 (Figure S3). Therefore, for each possible configuration we selected the conformation that shows the best agreement with the *J*-coupling data. These structures were further optimized using the density functional theory (DFT) calculations at the B3LYP/6-31G(d) level of theory.

Table 2. Numbering of 10 Possible Configurations for Unknown Stereocenters C1, C2, C9, C10, and C16 and Number of Conformers Obtained from Conformational Search

no.	configuration	no. of conformers	no.	configuration	no. of conformers
1	*R*S*R*R*R**	3	6	*R*S*S*S*S**	6
2	*R*S*R*R*S**	4	7	*S*S*R*R*R**	13
3	*R*S*R*S*R**	1	8	*S*S*R*S*R**	6
4	*R*S*R*S*S**	4	9	*S*S*S*R*R**	2
5	*R*S*S*R*S**	11	10	*S*S*S*S*R**	3

We fitted the 14 experimental RDCs on the DFT-optimized structures for the mentioned 10 possible configurations. Alignment tensor of each structure was calculated by singular value decomposition (SVD) method as implemented in the RDC module of the MSpin program.[20] Theoretically predicted RDCs were determined from the computed alignment tensor and further compared with the experimentally calculated ones. Among 10 possible configurations, configuration 8 (*S*S*R*S*R**) showed unequivocally the lowest *Q* factor[21] (*Q* = 0.08, Figure 3), with an excellent agreement between the experimental and back-calculated RDCs (Table S1 and Figure S4). All the other configurations have significantly larger *Q*-factors. Therefore, the relative configuration of **1** could be unambiguously assigned as 1*S**,2*S**,9*R**,10*S**,16*R**. Additionally, the unprecedented structure of tricyclo[11.3.0.0^{2,16}]-hexadecane carbon framework proposed by conventional NMR correlations could be conclusively affirmed by the RDC analysis.

Sarcomililate A (**1**) contains several rotatable bonds in the macrocyclic ring. Therefore, it is conceivable that the molecule is rather flexible, containing multiple main populated conformations. Nevertheless, DFT-optimized structure of *S*S*R*S*R** fits excellently to the experimental RDCs and *J*-couplings, indicating that this conformation exists as the major conformation in solution. It is important to note that we did not include the RDCs of C-11/H-11 and C-12/H-12 in the calculation of the alignment tensor, as they could not be extracted experimentally with high accuracy. Therefore, we cannot exclude the possibility that the corresponding parts of the structure are more dynamic. Additionally, two long-range NOEs (H-1/H-9, H-1/H-5, Figure S5) could be unambigu-

DOI: 10.1021/acs.joc.8b03020
J. Org. Chem. 2019, 84, 2568−2576

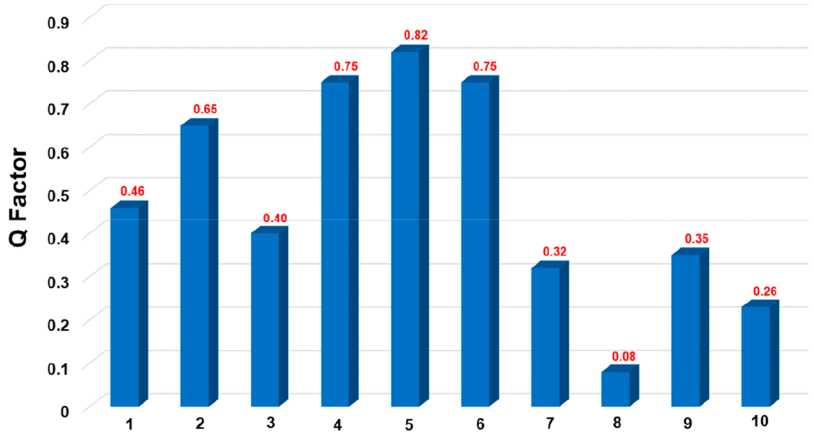

Figure 3. Comparison of *Q* factors of RDCs data of 10 possible configurations of **1**. The conformers for the RDCs analysis were optimized with DFT at the B3LYP/6-31G(d) level.

ously assigned, supporting the RDC-determined conformer (Figure 4) as the major conformation in solution.

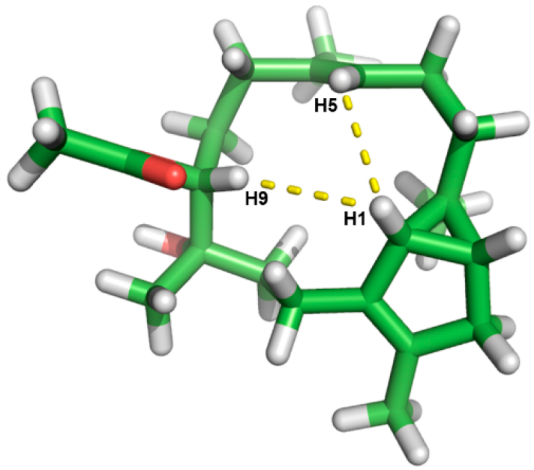

Figure 4. Long-range NOEs of H-1/H-9 and H-1/H-5 from zero-quantum NOESY spectrum that additionally confirmed the RDC-determined conformation of *S*S*R*S*R** as the major conformation.

To determine the absolute configuration of **1**, ECD spectra of both enantiomeric forms (1*S*,2*S*,9*R*,10*S*,16*R* and 1*R*,2*R*,9*S*,10*R*,16*S*) were computed by means of time-dependent density functional theory (TDDFT) calculations, using NMR-determined conformation as the initial structure input. The ECD calculations were conducted with the B3LYP/6-311G(d) basis set using the IEFPCM solvent continuum model with CH_3CN as the solvent. As shown in Figure 5, the experimental ECD spectrum of **1** in CH_3CN displayed two positive $\pi-\pi^*$ Cotton effects, at 204 nm ($\Delta\varepsilon$ + 2.92) and 217 nm ($\Delta\varepsilon$ + 3.57), respectively. Excellent agreement between the experimental ECD spectrum and the calculated one permitted the assignment of the absolute configuration as 1*S*,2*S*,9*R*,10*S*,16*R*.

In addition, the absolute configurations of C-9 and C-10 in compound **1** were further confirmed by Snatzke's method, of which compounds **1a** and **1b** (Figure 1) were successively synthesized. The NOE experiment of **1b** determined the erythro-configuration of the vicinal diol, allowing the application of Snatzke's method to confirm its absolute configuration by measuring the $Mo_2(OAc)_4$ induced circular spectrum (ICD) of Mo-complex of **1a** (see Supporting Information for the details). Finally, the 9*R*,10*S* configuration was confirmed by a negative sign of Cotton effect (CE) at 300 nm (Figure 6).[22−25]

By comparison of the obtained spectroscopic data with those reported in the literature, two of the other four isolated compounds (**2**−**5**) could be rapidly identified as yalongene A (**4**)[26] and sarcophytol M (**5**),[27] respectively.

Compound **2**, sarcomililatol A, was obtained as a colorless crystal (MeOH), mp 125−126 °C. Its molecular formula was assigned to be $C_{22}H_{36}NaO_4$ from the HR-ESI-MS at *m*/*z* 387.2506 ($[M + Na]^+$, calcd 387.2506), suggesting five degrees of unsaturation. The ^1H NMR spectrum showed six diagnostic singlets at δ_H 1.42, 1.43, 1.86, 1.60, 1.20, and 2.19, which could be assigned to C-16, C-17, C-18, C-19, C-20 methyls, and the acetyl, respectively. The typical downfield shifted broad doublet at δ_H 5.16 (J = 9.6 Hz) was assigned to an oxymethine bearing an acetoxy group. Detailed analysis of the $^1H-^1H$ COSY, in combination with HSQC and HMBC experiments, allowed all related signals in the ^1H- and ^{13}C NMR spectra to be assigned, which led to the establishment of the planar structure of **2**, featuring a 14-membered cembrane ring containing three double bonds at C-1, C-3, and C-7, two hydroxy groups at C-12 and C-15, and one acetoxy group at C-11. Moreover, because **2** was obtained as a suitable crystal, it was submitted to X-ray diffraction analysis using graphite-monochromated Cu Kα radiation (λ = 1.54178 Å). The X-ray structure shown in Figure 7 not only confirmed the deduced planar structure of **2** but also clearly disclosed its absolute configuration as 1*E*,3*E*,7*E*,11*S*,12*S* [with small Flack parameter −0.08 (10)]. It is worth noting that the assignment of the absolute configuration of the vicinal diol moiety (C-11 and C-12) in **2** is identical to that of C-9 and C-10 in **1**, determined by a combination of RDC-based NMR analysis and ECD calculations. Considering the fact that **1** and **2** were isolated from the same species and they showed high structural similarity in the macrocyclic rings, it is reasonably expected that **1** and **2** shared the same absolute configuration in the vicinal diol moiety.

Sarcomililatol B (**3**) was isolated as a white amorphous powder. Its molecular formula, $C_{20}H_{34}O_3$, was also established by HR-EI-MS showing an $[M]^+$ ion peak at *m*/*z* 322.2494 (calcd 322.2502), 42 mass units less than that of **2**. Overall comparison of ^1H- and ^{13}C NMR data of **2** and **3** revealed that

DOI: 10.1021/acs.joc.8b03020
J. Org. Chem. 2019, 84, 2568−2576

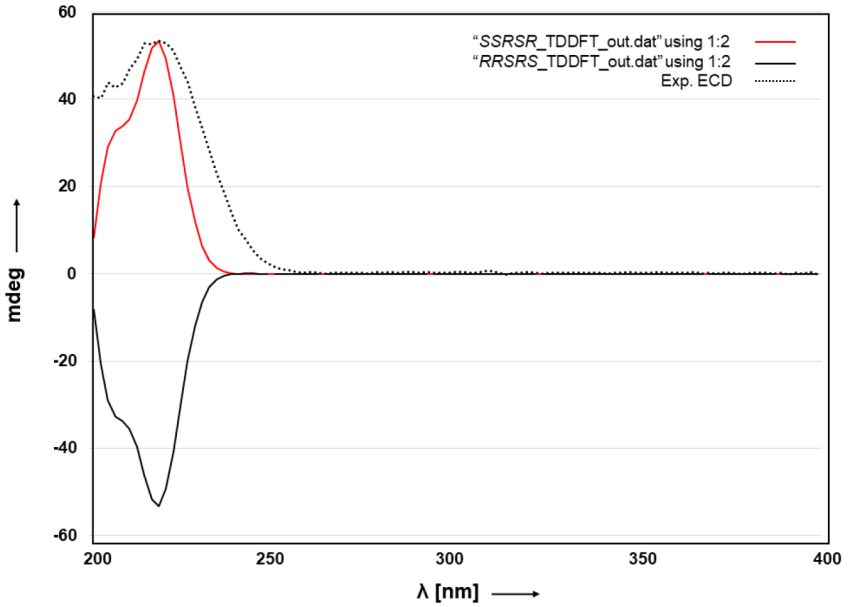

Figure 5. Comparison of experimental ECD spectrum (dashed) and DFT-predicted ECD spectra of 1*R*,2*R*,9*S*,10*R*,16*S* (black) and 1*S*,2*S*,9*R*,10*S*,16*R* (red). ECD spectra were predicted by means of time-dependent DFT calculations at the B3LYP/6-311G(d) level.

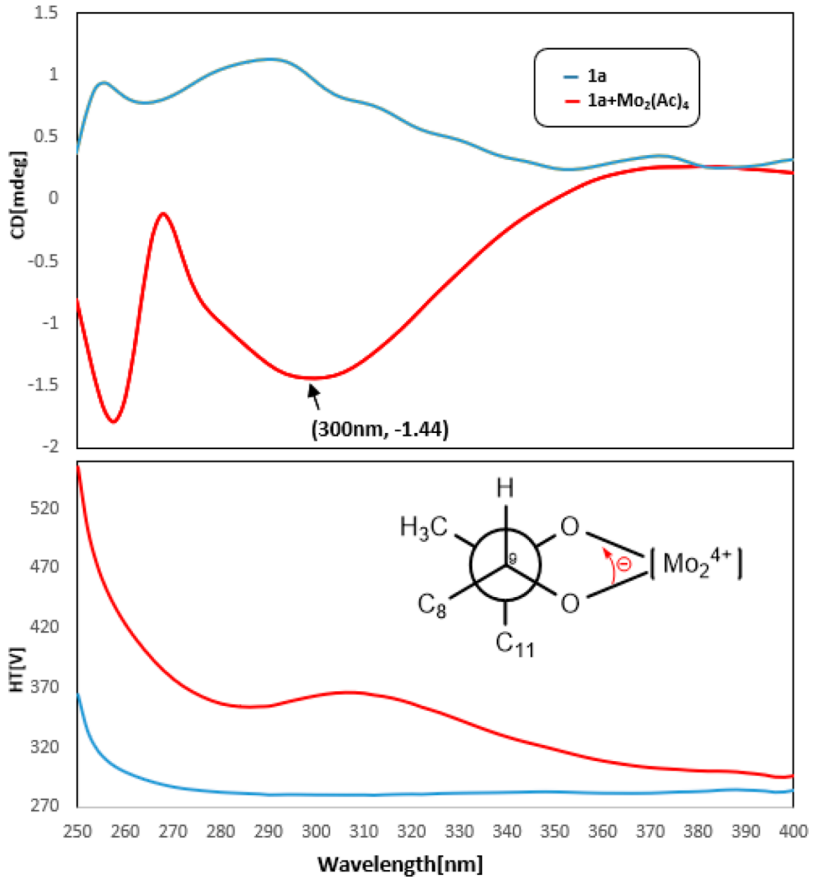

Figure 6. CD spectra and HT plots of **1a** and in situ formed Mo-complex of **1a** recorded in DMSO (the Newman projection represents the preferred conformation of the vicinal diol in the chiral Mo-complex).

the gross structure of **3** is almost identical with that of **2** (Table S2). In fact, the only difference between **2** and **3** happened at the substitution of C-11 position (the former is −OAc, and the latter is −OH). As the acetoxy group at C-11 in **2** was replaced by the hydroxy group in **3**, the chemical shift of H-11 was reasonably upfield shifted from δ_H 5.16 of **2** to δ_H 3.61 of **3**. Therefore, **3** is the C-11 deacetyl derivative of **2**.

It is worth pointing out that the NMR spectra of both **2** and **3** were recorded in CD_3OD (Table S2), instead of $CDCl_3$, because both compounds are extremely unstable in $CDCl_3$.

DOI: 10.1021/acs.joc.8b03020
J. Org. Chem. 2019, 84, 2568−2576

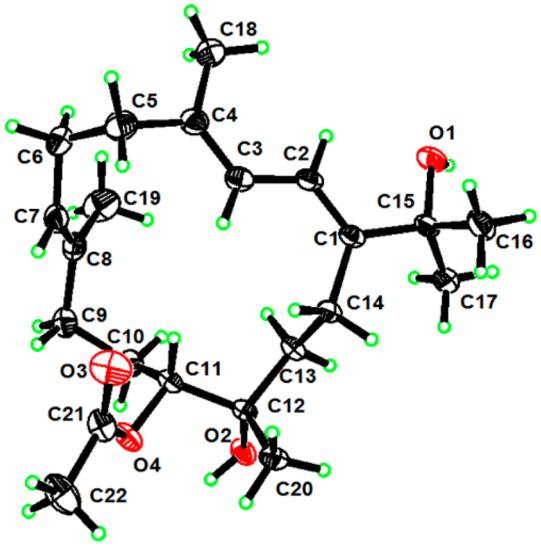

Figure 7. Perspective ORTEP drawing of X-ray structure of sarcomililatol A (**2**) (displacement ellipsoids are drawn at the 50% probability level).

Actually, when we initially recorded the NMR spectra of both **2** and **3** in $CDCl_3$, most probably due to the presence of trace HCl in $CDCl_3$, both compounds were transformed into two related compounds, **2a** and **3a**, respectively. The structure of **3a** was immediately recognized as sarglaucol, a cembrane-type diterpenoid previously isolated from the Hainan soft coral *Sarcophyton glaucum*.[28] Compound **2a** showed very similar ^{1}H- and ^{13}C NMR data as those of **3a** (Table S3), with the main difference being the NMR chemical shifts of C-11 ($\delta_{C/H}$ at 73.9/5.11 in **2a** and 71.3/3.65 in **3a**). This result clearly indicates that the hydroxy group at C-11 of **3a** was acetylated.[28] **2a** was thus determined as the acetylated product of **3a**.

The skeleton of sarcomililate A (**1**) is unprecedented and formally different from the co-occurring cembranoids **2**, **3**, and derived **2a**. Nevertheless, it is interesting to note that **1**−**3** and **2a** share a similar macrocycle bearing a trisubstituted double bond and a vicinal diol moiety. On the basis of the structural similarity of these molecules and the biogenetic consideration, we propose a plausible biosynthetic connection between them (Scheme 1 and Table S5): acetylation of **3** affords compound **2**, which is dehydrated under the acid condition to give the conjugated triene **2a**. Compound **2a** undergoes an isomerization, followed by an intramolecular [4 + 2] cycloaddition, to yield the novel diterpenoid **1**.

All the reported compounds were evaluated for various biological activities. In the cytotoxic assay, they were inactive on the cell lines of A549, HT-29, Hep3B, and MDA-MB-436 at the highest concentration of 50 μM. Meanwhile, in the immunological assay, all the compounds, including the novel sarcomililate A (**1**), were found to inhibit the proliferation of ConA-induced T lymphocyte cells and/or LPS-induced B lymphocyte cells in vitro, with IC_{50} values ranging from 4.8 to 49.8 μM (Table 3). Cyclosporin A (CsA) was used as the positive control. The results indicated that the lower degrees of oxidation might be crucial for the immunosuppressive activity of this compound class. Intriguingly, yalongene A (**4**), the hydrocarbon molecule, exhibited the strongest inhibition on the proliferation of LPS-induced B lymphocyte cells with IC_{50} value of 4.8 μM and selective index (SI) of 7.2 (better than CsA) (Table 3), providing a promising structure scaffold for the discovery of specific immunosuppressive agents with low toxicity.

Scheme 1. Proposed Biosynthetic Pathway of Compounds 1−3

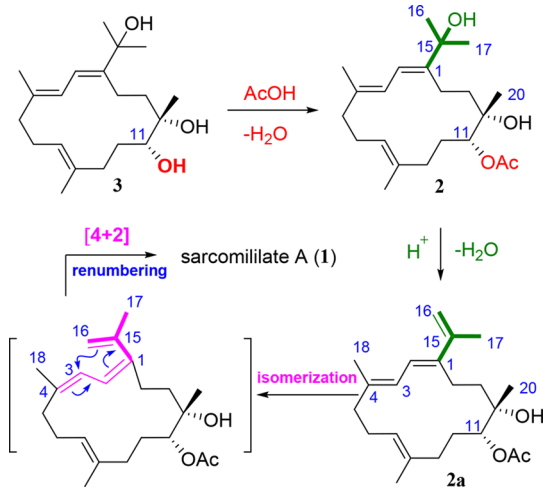

Table 3. Immunosuppressive Tests of Compounds 1−5

		ConA-induced T-cell proliferation		LPS-induced B-cell proliferation	
compd	CC_{50} (μM)	IC_{50} (μM)	SI[a]	IC_{50} (μM)	SI[a]
1	34.6	49.8	0.7	20.2	1.7
2	27.1	38.9	0.7	22.1	1.2
3	>50	>50		>50	
2a	33.5	44.5	0.8	18.7	1.8
3a	>50	>50		49.5	1.4
4	34.8	>50		4.8	7.2
5	6.2	11.4	0.5	4.9	1.2
CsA	1.2	0.04	30.0	0.4	3.0

[a]SI is determined as the ratio of the concentration of the compound that reduced cell viability to 50% (CC_{50}) to the concentration of the compound needed to inhibit the proliferation by 50% relative to the control value (IC_{50}).

CONCLUSION

In this study, we isolated and identified a novel diterpene sarcomililate A (**1**), which possesses an unprecedented tricyclo[11.3.0.0^{2,16}]hexadecane scaffold. The RDC-based NMR analysis was employed for establishing the relative configuration of five unknown stereogenic centers and the major populated conformation of **1**. Our study demonstrated the power of RDC-based analysis in the stereochemical elucidation of noncrystallizable natural products, in which the well-separated stereochemical domains cannot be correlated by NOEs and *J*-couplings. RDC-derived conformation of **1** was further used in the theoretical prediction of electronic circular dichroism (ECD) spectrum. Comparison of experimental and theoretical ECD spectra permitted unambiguous assignment of the absolute configuration of **1**, which has been further confirmed by Snatzke's method. Moreover, we also obtained and characterized two related new cembranoids, namely, sarcomililatols A and B (**2** and **3**), and two related known diterpenoids (**4** and **5**) from the title animal. Absolute configuration of **2** was unequivocally established by X-ray anomalous dispersion method using graphite-monochromated

DOI: 10.1021/acs.joc.8b03020
J. Org. Chem. 2019, 84, 2568−2576

Cu Kα radiation, giving further support for the assigned absolute configuration of **1** on a biogenetic aspect. Finally, based on the careful structural analysis, we proposed a plausible biogenetic relationship among **1**−**3** and **2a**, which nicely explained how these metabolites were biosynthesized. The discovery of sarcomililate A (**1**) has added to an extremely diverse and complex array of marine macrocyclic diterpenoids that is rapidly expanding. Now, there is a strong interest in performing further studies aimed at experimentally proving the true biogenetic origin and the effective biological role that sarcomililate A and related cembranoids play in the life cycle of soft corals and, finally, at confirming their structural peculiarities by synthesis.

EXPERIMENTAL SECTION

General Experimental Procedures. Optical rotation was measured on a PerkinElmer 241MC polarimeter. IR spectrum was recorded on a Nicolet6700 spectrometer (Thermo Scientific, Waltham, MA, U.S.A.). UV spectra were measured with a Cary 300-Bio UV−visible spectrometer (Varian, Palo Alto, CA, U.S.A.). CD spectra were measured on a JASCO J-810 instrument. NMR spectra were measured on a Bruker DRX-400, Bruker DRX-500, or Bruker DRX-600 spectrometer (Bruker Biospin AG, Fällanden, Germany). Chemical shifts (δ) are reported in ppm with reference to the solvent signals, and coupling constants (J) are in Hz. MS spectra were recorded on a Finnigan-MAT-95 mass spectrometer (FinniganMAT, San Jose, CA, U.S.A.). HR-ESI-MS data were detected on and recorded on an Agilent G6520 Q-TOF mass detector. Commercial silica gel (Qingdao Haiyang Chemical Group Co., Ltd., Qingdao, China, 200−300 and 400−600 mesh) and Sephadex LH-20 gel (Amersham Biosciences) were used for column chromatography, and precoated silica gel plates (Yan Tai Zi Fu Chemical Group Co., Yantai, China, G60 F-254) were used for analytical TLC. Reversed-phase (RP) HPLC was performed on an Agilent 1260 series liquid chromatograph equipped with a DAD G1315D detector at 210 and 254 nm. A semipreparative ODS-HG-5 column [5 μm, 250 × 9.4 mm] was employed for the purifications. Oligopeptide AAKLVFF was supplied by Professor Xinxiang Lei, purity >98%. Three mm NMR tubes and MeOD-d_4 solvent were bought from Deutero GMBH, Germany. All solvents used for CC and HPLC were of analytical grade (Shanghai Chemical Reagents Co., Ltd.) and chromatographic grade (Dikma Technologies, Inc.), respectively.

Biological Material. The specimens of *Sarcophyton mililatensis*, identified by Professor Hui Huang of the South China Sea Institute of Oceanology, Chinese Academy of Sciences (CAS), were collected by scuba at Xigu Island, Hainan Province, China, in May 2, 2014, at a depth of −20 m and were frozen immediately after collection. A voucher specimen is available for inspection at the Shanghai Institute of Materia Medica, CAS, under registration no. 14S-80.

Extraction and Isolation. The frozen animals (400 g, dry weight) were cut into pieces and extracted exhaustively with acetone at room temperature (3 × 1.5 L). The organic extract was evaporated to give a residue that was partitioned between Et_2O and H_2O. The Et_2O solution was concentrated under reduced pressure to give a dark-brown residue (13.5 g) that was fractionated by gradient Si gel column chromatography [0−100% Et_2O in petroleum ether (PE)], yielding 21 fractions. Fraction 16 was further purified by Sephadex LH-20 [PE/CH_2Cl_2/MeOH (2:1:1)], followed by sillica gel column chromatography [PE/acetone (3:1)], RP-HPLC [MeOH/H_2O (85:15), 3.0 mL/min] to give compound **1** (4.8 mg). Fraction 17 was further purified by Sephadex LH-20 [CH_2Cl_2/MeOH (1:1)], followed by silica gel column chromatography [PE/acetone (3:1)] to give compound **2** (18.0 mg), and fraction 19 was further purified by Sephadex LH-20 [CH_2Cl_2/MeOH (1:1)], followed by sillica gel column chromatography [PE/acetone (7:3)] to give compound **3** (5.1 mg). Fraction 1 was further purified by RP-HPLC [MeCN/H_2O (90:10), 3.0 mL/min] to give compound **4** (2.3 mg). Fraction 6 was further purified by Sephadex LH-20 [PE/CH_2Cl_2/MeOH (2:1:1)], followed by sillica gel column chromatography [PE/diethyl ether (9:1)] to give compound **5** (3.5 mg).

*Sarcomililate A (**1**).* Colorless oil; $[\alpha]_D^{25}$ +42 (c 0.10, MeOH); ECD (MeCN) 217 nm ($\Delta\varepsilon$ + 3.57); IR ν_{max}: 3456, 2955, 2922, 2871, 2847, 1733, 1436, 1375, 1243, 1196, 1180, 1132, 1076, 1023 cm^{-1}; ^{1}H and ^{13}C NMR data, see Table 1 in the manuscript; HR-EI-MS m/z 346.2507 [M]$^+$ (calcd for $C_{22}H_{34}O_3$, 346.2502).

*Sarcomililatol A (**2**).* Colorless crystals; mp 125−126 °C; $[\alpha]_D^{25}$ −254 (c 0.25, $CHCl_3$); UV (MeOH) λ_{max} (log ε) 250 (3.97); IR ν_{max}: 3444, 2974, 2931, 2855, 1732, 1451, 1373, 1241, 1132, 1077, 1027 cm^{-1}; ^{1}H and ^{13}C NMR data, see Table S2; HR-ESI-MS m/z 387.2506 [M + Na]$^+$ (calcd for $C_{22}H_{36}NaO_4$, 387.2506).

*Sarcomililatol B (**3**).* White powder; $[\alpha]_D^{25}$ −82 (c 0.10, $CHCl_3$); UV (MeOH) λ_{max} (log ε) 248 (3.75); IR ν_{max}: 3389, 2971, 2928, 2858, 1196, 1180, 1142, 1132, 1076 cm^{-1}; ^{1}H and ^{13}C NMR data, see Table S2; HR-EI-MS m/z 322.2494 [M]$^+$ (calcd for $C_{20}H_{34}O_3$, 322.2502).

X-ray Crystal Structure Analysis of 2. Compound **2** was crystallized from mixed solvents of petroleum ether, diethyl ether, and methanol at room temperature. The X-ray crystallographic data for compound **2** were obtained on a Bruker APEX-II CCD diffractometer employing graphite monochromated Cu Kα radiation (wavelength = 1.54178 Å) at 205 K. The structures were solved by direct method using ShelXT (Sheldrick, 2015) and refined with full-matrix least-squares calculations on F2 using SHELXL (Sheldrick, 2015). All non-hydrogen atoms were refined anisotropically. The hydrogen atom positions were geometrically idealized and allowed to ride on their parent atoms.

Crystallographic data for sarcomililatol A (**2**) have been deposited at the Cambridge Crystallographic Data Center with the deposition number of CCDC 1860765 for sarcomililatol A (**2**). A copy of the data can be obtained free of charge on application to the CCDC, 12 Union Road, Cambridge CB21EZ, U.K. [tel.: (+44)1223-336-408; fax: (+44) 1223-336-033; e-mail: deposit0@ccdc.cam.ac.uk]. X-ray powder diffraction analysis of compound **2** is also available.

Immunosuppressive Activity Assay.[29] *Materials.* Stock solutions of compounds were dissolved with 100% dimethyl sulfoxide (DMSO, Sinopharm, China) and diluted with RPMI 1640 medium (Hyclone, South Logan, UT, U.S.A.) containing 10% fetal bovine serum (FBS). Cell Counting Kit-8 (CCK-8) was purchased from Dojindo (Kumamoto, Japan). Concanavalin A (Con A) and lipopolysaccharide (LPS, *Escherichia coli* 055:B5) were purchased from Sigma (St Louis, MO, U.S.A.).

Animals. Inbred 6−8-week-old female BALB/c mice were purchased from Shanghai Lingchang Biotechnology Co., Ltd. (certificate no. 2013-0018). The mice were housed under specific pathogen-free conditions with a controlled environment (12 h of light/12 h of dark cycle, 22 ± 1 °C, 55 ± 5% relative humidity). All mice were fed standard laboratory chow and water ad libitum. All mice were allowed to acclimatize in our facility for 1 week before any experiment started. All experiments were carried out according to the National Institutes of Health Guide for Care and Use of Laboratory Animals and were approved by the Bioethics Committee of the Shanghai Institute of Materia Medica.

Splenocytes Preparation. Mice were sacrificed, and their spleens were removed aseptically. The spleens were ground up, and a single-cell suspension was prepared after cell debris and clumps were removed. Erythrocytes were depleted with ammonium chloride buffer solution. Cells were washed and resuspended in RPMI 1640 media containing 10% FBS, penicillin (100 U/mL), and streptomycin (100 μg/mL). Cells were counted by trypan blue exclusion.

Cell Viability Assay. Splenocytes (1 × 10^6 cells) were cultured in 96-well plates in triplicate with 200 μL of RPMI 1640 media containing 10% FBS, penicillin (100 U/mL), and streptomycin (100 μg/mL) in a humidified, 37 °C, 5% CO_2-containing incubator for 48 h in the presence or absence of indicated concentrations of compounds. A total of 20 μL of CCK-8 was added to each well. After 6−8 h incubation, the absorbance value at 450 nm (570 nm

DOI: 10.1021/acs.joc.8b03020
J. Org. Chem. 2019, 84, 2568−2576

calibration) was collected by a microplate reader (Molecular Devices, Sunnyvale, CA, U.S.A.) and the cell viability was calculated.

Con A and LPS-Induced Proliferation Assay. Splenocytes (5×10^5 cells) were cultured in triplicate for 48 h and stimulated with 5 μg/mL of Con A or 10 μg/mL of LPS in the presence or absence of the indicated concentrations of compounds. The cell cultures were then incubated in a humidified, 37 °C, 5% CO_2-containing incubator. Cells were pulsed with 0.5 μCi/mL of [^{3}H]thymidine for 8 h and harvested onto glass fiber filters. The incorporated radioactivity was counted using a Beta Scintillation Counter (MicroBeta Trilux, PerkinElmer Life Sciences, Boston, MA).

■ ASSOCIATED CONTENT

Supporting Information

The Supporting Information is available free of charge on the ACS Publications website at DOI: 10.1021/acs.joc.8b03020.

RDC-based NMR analysis of **1**; the ECD calculations of **1**; the $Mo_2(OAc)_4$ induced circular dichroism experiment of **1a**; the crystallographic data of **2**; and the 1D and 2D NMR, HRMS, and IR spectra of **1**−**5** (PDF)

Crystal data for **2** in CIF format (CIF)

■ AUTHOR INFORMATION

Corresponding Authors

*E-mail: xwli@simm.ac.cn.
*E-mail: hsun@fmp-berlin.de.
*E-mail: ywguo@simm.ac.cn.

ORCID

Jian-Rong Wang: 0000-0002-0853-7537
Xu-Wen Li: 0000-0001-7919-9726
Yue-Wei Guo: 0000-0003-0413-2070

Author Contributions

⊥M.Y. and X.-L.L. contributed equally.

Notes

The authors declare no competing financial interest.

Crystallographic data for sarcomililatol A (**2**) have been deposited at the Cambridge Crystallographic Data Center with the deposition number of CCDC 1860765 for sarcomililatol A (**2**). A copy of the data can be obtained free of charge on application to the CCDC, 12 Union Road, Cambridge CB21EZ, U.K. [Tel.: (+44)1223-336-408; fax: (+44) 1223-336-033; e-mail: deposit0@ccdc.cam.ac.uk]. X-ray powder diffraction analysis of compound **2** is also available.

■ ACKNOWLEDGMENTS

This research work was financially supported by the National Key Research and Development Program of China (no. 2018YFC0310903), the Drug Innovation Major Project (no. 2018ZX09711-001-001-009), the National Natural Science Foundation of China (NSFC) (nos. 81520108028, 21672230, and 81603022), and the SKLDR/SIMM Project (no. SIMM1705ZZ-01). H.S. and X.-L.L. thank the Sino-German Center for Research Promotion (GZ1289) for financial support. X.-W.L. is thankful for the financial support of "Youth Innovation Promotion Association" (no. 2016258) from Chinese Academy of Sciences and SA-SIBS Scholarship Program. We thank Prof. X.-B. Li from Hainan University for the taxonomic identification of the soft coral material and Dr. T. Kurtán for the helpful discussion about absolute configuration determination using TDDFT-ECD.

■ REFERENCES

(1) Liang, L.-F.; Guo, Y.-W. Terpenes from the Soft Corals of the Genus *Sarcophyton*: Chemistry and Biological Activities. *Chem. Biodiversity* **2013**, *10*, 2161−2196.

(2) Li, S.-W.; Ye, F.; Zhu, Z.-D.; Huang, H.; Mao, S.-C.; Guo, Y.-W. Cembrane-Type Diterpenoids from the South China Sea Soft Coral *Sarcophyton mililatensis*. *Acta Pharm. Sin. B* **2018**, *8*, 944−955.

(3) Liang, L.-F.; Chen, W.-T.; Li, X.-W.; Wang, H.-Y.; Guo, Y.-W. New Bicyclic Cembranoids from the South China Sea Soft Coral *Sarcophyton trocheliophorum*. *Sci. Rep.* **2017**, *7*, 46584.

(4) Chen, W.-T.; Li, J.; Wang, J.-R.; Li, X.-W.; Guo, Y.-W. Structural Diversity of Terpenoids in the Soft Coral *Sinularia flexibilis*, Evidenced by A Collection from the South China Sea. *RSC Adv.* **2015**, *5*, 23973−23980.

(5) Liang, L.-F.; Kurtán, T.; Mándi, A.; Gao, L.-X.; Li, J.; Zhang, W.; Guo, Y.-W. Sarsolenane and Capnosane Diterpenes from the Hainan Soft Coral *Sarcophyton trocheliophorum* Marenzeller as PTP1B Inhibitors. *Eur. J. Org. Chem.* **2014**, *2014*, 1841−1847.

(6) Kurtán, T.; Jia, R.; Li, Y.; Pescitelli, G.; Guo, Y.-W. Absolute Configuration of Highly Flexible Natural Products by the Solid-State ECD/TDDFT Method: Ximaolides and Sinulaparvalides. *Eur. J. Org. Chem.* **2012**, *2012*, 6722−6728.

(7) Yan, X.-H.; Gavagnin, M.; Cimino, G.; Guo, Y.-W. Two New Biscembranes with Unprecedented Carbon Skeleton and Their Probable Biogenetic Precursor from the Hainan Soft Coral *Sarcophyton latum*. *Tetrahedron Lett.* **2007**, *48*, 5313−5316.

(8) Ye, F.; Li, J.; Wu, Y.; Zhu, Z.-D.; Mollo, E.; Gavagnin, M.; Gu, Y.-C.; Zhu, W.-L.; Li, X.-W.; Guo, Y.-W. Sarinfacetamides A and B, Nitrogenous Diterpenoids with Tricyclo[6.3.1.0^{1,5}]dodecane Scaffold from the South China Sea Soft Coral *Sarcophyton infundibuliforme*. *Org. Lett.* **2018**, *20*, 2637−2640.

(9) Ye, F.; Zhu, Z.-D.; Chen, J.-S.; Li, J.; Gu, Y.-C.; Zhu, W.-L.; Li, X.-W.; Guo, Y.-W. Xishacorenes A−C, Diterpenes with Bicyclo[3.3.1]nonane Nucleus from the Xisha Soft Coral *Sinularia polydactyla*. *Org. Lett.* **2017**, *19*, 4183−4186.

(10) Liang, L.-F.; Kurtán, T.; Mándi, A.; Yao, L.-G.; Li, J.; Zhang, W.; Guo, Y.-W. Unprecedented Diterpenoids as a PTP1B Inhibitor from the Hainan Soft Coral *Sarcophyton trocheliophorum* Marenzeller. *Org. Lett.* **2013**, *15*, 274−277.

(11) Liu, Y.-Z.; Saurí, J.; Mevers, E.; Peczuh, M. W.; Hiemstra, H.; Clardy, J.; Martin, G. E.; Williamson, R. T. Unequivocal Determination of Complex Molecular Structures Using Anisotropic NMR Measurements. *Science* **2017**, *356* (6333), eaam5349.

(12) Milanowski, D. J.; Oku, N.; Cartner, L. K.; Bokesch, H. R.; Williamson, R. T.; Saurí, J.; Liu, L.-Z.; Blinov, K. A.; Ding, Y.-Q.; Li, X.-C.; Ferreira, D.; Walker, L. A.; Khan, S.; Davies-Coleman, M. T.; Kelley, J. A.; McMahon, J. B.; Martin, G. E.; Gustafson, K. R. Unequivocal Determination of Caulamidines A and B: Application and Validation of New Tools in the Structure Elucidation Tool Box. *Chem. Sci.* **2018**, *9*, 307−314.

(13) Navarro-Vázquez, A.; Gil, R. R.; Blinov, K. Computer-Assisted 3D Structure Elucidation (CASE-3D) of Natural Products Combining Isotropic and Anisotropic NMR Parameters. *J. Nat. Prod.* **2018**, *81*, 203−210.

(14) Schmidts, V.; Fredersdorf, M.; Lübken, T.; Porzel, A.; Arnold, N.; Wessjohann, L.; Thiele, C. M. RDC-Based Determination of the Relative Configuration of the Fungicidal Cyclopentenone 4,6-Diacetylhygrophorone A12. *J. Nat. Prod.* **2013**, *76*, 839−844.

(15) Ge, H.-M.; Sun, H.; Jiang, N.; Qin, Y.-H.; Dou, H.; Yan, T.; Hou, Y.-Y.; Griesinger, C.; Tan, R.-X. Relative and Absolute Configuration of Vatiparol (1 mg): A Novel Anti-inflammatory Polyphenol. *Chem. - Eur. J.* **2012**, *18*, 5213−5221.

(16) Li, G.-W.; Liu, H.; Qiu, F.; Wang, X.-J.; Lei, X.-X. Residual Dipolar Couplings in Structure Determination of Natural Products. *Nat. Prod. Bioprospect.* **2018**, *8*, 279−295.

(17) Lei, X.-X.; Qiu, F.; Sun, H.; Bai, L.; Wang, W.-X.; Xiang, W.-S.; Xiao, H.-P. A Self-Assembled Oligopeptide as A Versatile NMR Alignment Medium for the Measurement of Residual Dipolar

DOI: 10.1021/acs.joc.8b03020
J. Org. Chem. 2019, 84, 2568−2576

Couplings in Methanol. *Angew. Chem., Int. Ed.* **2017**, *56*, 12857−12861.
(18) Enthart, A.; Freudenberger, J. C.; Furrer, J.; Kessler, H.; Luy, B. The CLIP/CLAP-HSQC: Pure Absorptive Spectra for the Measurement of One-Bond Couplings. *J. Magn. Reson.* **2008**, *192*, 314−322.
(19) *Small-Molecule Drug Discovery Suite 2017*; Schrödinger, LLC: New York, 2017.
(20) Navarro-Vázquez, A. MSpin-RDC. A Program for the Use of Residual Dipolar Couplings for Structure Elucidation of Small Molecules. *Magn. Reson. Chem.* **2012**, *50*, S73−S79.
(21) Cornilescu, G.; Marquardt, J. L.; Ottiger, M.; Bax, A. Validation of Protein Structure from Anisotropic Carbonyl Chemical Shifts in a Dilute Liquid Crystalline Phase. *J. Am. Chem. Soc.* **1998**, *120*, 6836−6837.
(22) Snatzke, G.; Wagner, U.; Wolff, H. P. Circular Dichroism. LXXV. Cottonogenic Derivatives of Chiral Bidentate Ligands with the Complex $[Mo_2(O_2CCH_3)_4]$. *Tetrahedron* **1981**, *37*, 349−361.
(23) Frelek, J.; Geiger, M.; Voelter, W. Transition Metal Complexes as Auxiliary Chromophores in Chiroptical Studies on Carbohydrates. *Curr. Org. Chem.* **1999**, *3*, 117−146.
(24) Górecki, M.; Jabłońska, E.; Kruszewska, A.; Suszczyńska, A.; Urbańczyk-Lipkowska, Z.; Gerards, M.; Morzycki, J. W.; Szczepek, W. J.; Frelek, J. Practical Method for the Absolute Configuration Assignment of tert/tert 1,2-Diols Using Their Complexes with $Mo_2(OAc)_4$. *J. Org. Chem.* **2007**, *72*, 2906−2916.
(25) Di Bari, L.; Pescitelli, G.; Pratelli, C.; Pini, D.; Salvadori, P. Determination of Absolute Configuration of Acyclic 1,2-Diols with $Mo_2(OAc)_4$. 1. Snatzke's Method Revisited. *J. Org. Chem.* **2001**, *66*, 4819−4825.
(26) Yao, L.-G.; Zhang, H.-Y.; Liang, L.-F.; Guo, X.-J.; Mao, S.-C.; Guo, Y.-W. Yalongenes A and B, Two New Cembranoids with Cytoprotective Effects from the Hainan Soft Coral *Sarcophyton trocheliophorum* Marenzeller. *Helv. Chim. Acta* **2012**, *95*, 235−239.
(27) Kobayashi, M.; Osabe, K. Marine Terpenes and Terpenoids. VII. Minor Cembranoid Derivatives, Structurally Related to the Potent Anti-Tumor-Promoter Sarcophytol A, from the Soft Coral *Sarcophyton glaucum*. *Chem. Pharm. Bull.* **1989**, *37*, 631−636.
(28) Zhang, C.-X.; He, X.-X.; Zhang, J.; Guo, Q.; Lei, L.-F.; Su, J.-Y.; Zeng, L.-M. New Precursor of Tetraterpenoids from the Soft Coral *Sarcophyton glaucum*. *Nat. Prod. Res.* **2013**, *27*, 782−786.
(29) Zhang, Q.-M.; Zhang, L.-Y.; Yu, J.; Li, H.; He, S.-J.; Tang, W.; Zuo, J.-P.; Lu, W. Discovery of New BTK Inhibitors with B Cell Suppression Activity Bearing A 4,6-Substituted Thieno[3,2-d]-pyrimidine Scaffold. *RSC Adv.* **2017**, *7*, 26060−26069.

DOI: 10.1021/acs.joc.8b03020
J. Org. Chem. 2019, 84, 2568−2576